U. S. DEPARTMENT OF THE INTERIOR
U. S. GEOLOGICAL SURVEY

CROSS-WELL RADAR IN LAYERED SEDIMENTS

by

Karl J. Ellefsen[1]

Open File Report 96-510

---

[1] U. S. Geological Survey, MS 964, Box 25046, Denver, CO 80225

1996

ABSTRACT

At the M-Area basin, Savannah River Site, the saturated and the unsaturated zones have been contaminated with dense non-aqueous phase liquids. To decrease the cost of and the time required for remediation of the contaminated sediments and ground water, some means of monitoring the remediation is needed. One promising technology is cross-well radar: the results of field experiments have shown that radar waves are strongly affected by sediments containing dense non-aqueous phase liquids. To use cross-well radar for monitoring, a sound understanding of how radar waves propagate in layered media is needed; for this reason, a theoretical study was performed.

For the study, the layered sediments were represented with a model having three layers: clay, sand, and clay. Radar scans were calculated for three antenna configurations that are commonly used for aquiring cross-well data, and the interpretations of those scans were substantiated with an analysis using mode theory. In general, the results indicate that the radar wave detected by the receiving antenna will have a relatively small amplitude when one or both antennas are in the clay layer but will have a relatively large amplitude when both antennas are in the sand layer. For the latter antenna configuration, the travel times can be used to estimate a bulk dielectric permittivity for the sand layer. The amplitudes, however, cannot be related in a simple, straightforward manner to the properties of the sand layer because they are affected by the properties of all three layers.

To predict the suitability of cross-well radar for monitoring the remediation at Savannah River Site, radar wave propagation in models representing contaminated sediments must be simulated; such work will be in a subsequent report. This study was a crucial, necessary step towards that goal.

CONTENTS

LIST OF FIGURES

LIST OF TABLES

1. INTRODUCTION

At Savannah River Site, which is near Aiken, South Carolina, approximately 2 million pounds of dense non-aqueous phase liquids were put into the "M-Area Settling Basin" (Westinghouse Savannah River Company, 1992, p. 2) whence they migrated into the unsaturated and the saturated zones. To decrease the cost and improve the efficiency of remediating the contaminated soils and ground water, some means of monitoring the remediation is needed (Jordan and others, 1993). To this end, the U. S. Geological Survey, which is being sponsored by the U. S. Department of Energy, is testing different geophysical methods at the Site. One method, cross-well radar, is particularly promising as the results of field experiments have demonstrated that radar waves are strongly affected by sediments containing dense non-aqueous phase liquids (Greenhouse and others, 1993).

At the Site, the saturated and the unsaturated zones consist of stratified, unconsolidated sands and clays, and this geology strongly affected the cross-well radar data collected there (Ellefsen, 1996a). For instance, radar waves were not detected where the sediments contain much clay, but high amplitude waves were detected where the sediments contain little clay. Sometimes, the character of the radar waves changed significantly as the antennas moved up the wells, and these changes are believed to be a manifestation of guided waves that are caused by the layering of the sediments.

The ultimate goal is to use cross-well radar to monitor changes in the fluids, which would occur during clean-up of dense non-aqueous phase liquids. The first step towards that goal is understanding how radar waves propagate in layered media because the sediments at the Site are layered and the dense non-aqueous phase liquids are believed to be concentrated in thin layers just above the clays (Westinghouse Savannah River Company, 1992, p. 2). As no information on this topic was found in the technical literature, a theoretical investigation was performed, and the findings are presented here. These findings were used to analyze the data collected at the Site (Ellefsen, 1996a) and to predict how the radar waves would be affected by changes in the fluids (Ellefsen, 1996b).

2. METHODS

The simplest model that could be used to investigate radar wave propagation in layered sediments consists of a sand layer between two clay layers. Each layer is assumed to be homogeneous and isotropic; the constitutive parameters for each layer are assumed to be linear and independent of frequency. The latter assumption is difficult to justify because the constitutive parameters for typical soils and sediments are known to depend upon frequency (see, for example, Hoekstra and Delaney, 1974). The problem with including such dependence is that it causes dispersion in addition to that caused by the conductivity and by the wave guide. Including this additional source of dispersion would make the results more difficult to analyze than they were, and for this reason, it was omitted. The wells are not included in the model. The transmitting and the receiving antennas are dipoles with infinitesimal length. Of course, all antennas have finite length, but, because such antennas may be represented as a series of antennas having infinitesimal length

(Stratton, 1941, p. 438-444), analyzing the latter case is enough for a thorough understanding of the wave behavior.

The model used in early attempts to analyze electromagnetic wave propagation in the atmosphere (see Wait, 1962, p. 132-143) is identical to that used in this study, and consequently the analytical solutions derived for the atmospheric problem can be used here. For the model (Figure 1), each layer is labeled 1, 2, or 3; for layer j, the relative dielectric permittivity is ε_{rj}, the relative magnetic permeability is μ_{rj}, and the conductivity is σ_j; the thickness of the middle layer is h. A vertical electric dipole, which simulates the transmitting antenna, is in the middle layer at a distance z_t from the interface between layers 1 and 2. The dipole moment is $I(\omega)\, ds / i\, \omega$ where $I(\omega)$ is the current, ds is the infinitesimal dipole length, ω is the angular frequency, and i is $\sqrt{-1}$. For this model, circular cylindrial coordinates for which the z axis is alligned with the dipole are appropriate; the model has azimuthal symmetry. The solution for the electromagnetic fields is found in the frequency-wavenumber domain using a Hertz potential Π that has only a z component. After transformation to the time-space domain, the potentials for the layers are:

$$\Pi_1(r,z,t) = \int_{-\infty}^{\infty} d\omega\, e^{i\omega t} \int_0^{\infty} A_1(k_r,\omega) e^{ik_{1z}z} J_0(k_r r) k_r\, dk_r, \tag{1}$$

$$\Pi_2(r,z,t) = \int_{-\infty}^{\infty} d\omega\, e^{i\omega t} \int_0^{\infty} \left[A_2(k_r,\omega) e^{ik_{2z}z} + B_2(k_r,\omega) e^{-ik_{2z}z} \right] J_0(k_r r) k_r\, dk_r +$$

$$\int_{-\infty}^{\infty} d\omega\, e^{i\omega t} \frac{I(\omega) ds}{4\pi(\sigma_2 + i\omega\varepsilon_{r2}\varepsilon_0)} \frac{e^{-ik_2\sqrt{r^2+(z-z_t)^2}}}{\sqrt{r^2+(z-z_t)^2}}, \text{ and} \tag{2}$$

$$\Pi_3(r,z,t) = \int_{-\infty}^{\infty} d\omega\, e^{i\omega t} \int_0^{\infty} B_3(k_r,\omega) e^{-ik_{3z}z} J_0(k_r r) k_r\, dk_r \tag{3}$$

(Wait, 1962, p. 138; Tyras, 1969, p. 173; Fuller and Wait, 1976, p. 244). The radial component of the wave number is k_r; the vertical component of the wave number for layer j is k_{jz}; and the dielectric permittivity of free space is ε_0. The coefficients A_1, A_2, B_2, and B_3 are calculated from the boundary conditions at each interface: Across each interface, the tangential components of the electric and magnetic field intensities must be continuous; these two conditions lead to two equations. With two interfaces, there are a total of four equations, which may be expressed in matrix form:

$$\mathbf{M}\begin{pmatrix} A_1 \\ A_2 \\ B_2 \\ B_3 \end{pmatrix} = \mathbf{b} \tag{4}$$

(see Tyras, 1969, p. 172). The elements in vector **b** are associated with the wave field radiated by the dipole; the elements in matrix **M** are associated with the wave field that interacts with the three layers.

Because the receiving antenna senses the vertical component of the electric field, the solution is desired in terms of that quantity, which for layer j is

$$E_{jz}(r,z,\omega) = \left(\frac{\partial^2}{\partial z^2} + k_j^2\right)\Pi_j(r,z,\omega), \tag{5}$$

where k_j is the wave number for layer j. To calculate radar scans, the integrals over radial wave number are computed via the discrete wave number method (Bouchon, 1981), and the integrals over frequency via fast Fourier transforms.

The second integral in equation 2 represents the wave field that propagates directly between the transmitting and the receiving antennas, and consequently this wave field will be called the direct wave. The first integral in equation 2 and the integrals in equations 1 and 3 represent another wave field caused by the interaction of the radiated wave field with the three layers. When r is large compared to h and when suitable constitutive parameters are chosen for the layers, this wave field behaves as if it were guided along layer 2 and consequently will be called the guided wave. Notice that the two wave fields can be calculated separately.

An invaluable method for gaining a deeper understanding of the behavior of the guided wave is to examine the mathematical expressions for it in the frequency domain. Here, each expression consists of only one integral over real radial wave number. If this integral is evaluated with contour integration in the complex radial wave number plane (Churchill and others, 1960, p. 170-194), then the vertical component of the electric field for layer j is

$$E_{jz}(r,z,\omega) = 2\pi i \sum_l R_l(r,z,\omega), \tag{6}$$

where R_l is the residue, which, in physical terms, is the contribution to the field from one mode. (The branch cut integrals, which are usually encountered in contour integration, are zero for this particular formulation (Tyras, 1969, p. 176).) The contribution is weighted

according to the locations of the transmitting and the receiving antennas. A mode, being simply a wave that satisfies the boundary conditions, is completely independent of the antenna locations; consequently, the matrix equation for the boundary conditions is

$$\mathbf{M}\begin{pmatrix} A_1 \\ A_2 \\ B_2 \\ B_3 \end{pmatrix} = \mathbf{0}. \tag{7}$$

(Essentiall, the elements in vector **b** of equation (4) which are associated with the radiating dipole are set to zero.) The equation has a non-trivial solution if

$$\det(\mathbf{M}) = 0, \tag{8}$$

which is often called either the period equation or the dispersion equation. Each value of complex k_r for which this equation is satisfied is uniquely associated with one mode. The real part of k_r is used to compute the phase velocity of the mode:

$$v = \frac{\mathrm{Re}(k_r)}{\omega}; \tag{9}$$

the imaginary part of k_r simply equals the attenuation factor of the mode.

The electromagnetic fields for a mode vary with z; in other words, they have a characteristic spatial pattern or shape. To determine a shape, the elements in matrix **M** are computed using the complex k_r for the desired mode. The coefficients A_1, A_2, B_2, and B_3 are then computed using equation (7): since this matrix equation is over-determined, one coefficient is set to some arbitrary value, and then the relative values of the other coefficients are computed. These coefficients are then used in the equations for the electromagnetic fields (for example, equation 5) to compute the shape. Shapes of different modes at the same frequency or shapes of the same mode at different frequencies may be compared, but the magnitudes of the fields associated with those shapes may not be compared because they depend upon the cofficient that was set.

An important property of a mode is the velocity at which its energy propagates because that velocity determines the travel time. The energy velocity is computed via

$$v_e = \frac{P}{W_m + W_e} \tag{10}$$

where P is the time-average power flow, W_m is the time-average magnetic energy per unit radial length, and W_e is the time-average electric energy per unit radial length (Collin,

1991, p. 338). These three quantities are computed using the mode shapes; the effects of the relative magnitude of the field, which occurs because one coefficient is set to an arbitrary value, are removed because of the ratio in this equation.

For one example in the next section, radar scans were calculated when both antennas were in layer 1 and when both were in layer 3. Because the mathematical expressions for the Hertz potentials in these two cases are only slightly different from those in equations 1, 2, and 3 and because the potentials and the associated derivations are in Wait (1962, p. 35-39), they will not be repeated here.

3. RESULTS

In the prevous section, the mathematical solution for electromagnetic wave propagation when the transmitting and the receiving antennas were in the same layer included a direct wave and a guided wave. The behavior of the direct wave may be readily predicted because it can be expressed as a summation of plane waves (Stratton, 1941, p. 577-578), of which the behavior has already been thoroughly studied (see, for example, Stratton, 1941, p. 268-340). Consequently, the direct wave will only be cursorily investigated here. In contrast, the behavior of the guided wave in layered sediments has not been studied, and for this reason much of this section will focus on the behavior of this wave. The investigation will use mode theory extensively.

3.1 General Properties of the Modes

The properties of the modes were calculated for a model representing saturated sediments (Table 1). Layers 1 and 3, which represent clays, have identical properties. The frequencies varied from 1 to 500 MHz, which is broad enough to include the operating ranges of almost all borehole radar equipment currently available. Within this frequency range are many modes; only the properties of the first fifteen (Figure 2) were calculated as that is enough to demonstrate the behavior of all the others. The modes are numbered in increasing order starting with 0; mode 0 is sometimes called the fundamental mode, and the others the higher-order modes. The properties of the modes will be compared to the properties of two plane waves propagating in infinite homogenous media: for one wave the medium has the constitutive parameters of the sand layer, and for the other wave the parameters of the clay layer.

At high frequencies, the energy velocities (Figure 2a) asymptotically approach and are always less than the energy velocity of the plane wave in the sand medium. At low frequencies, the energy velocities decrease significantly, and those for the higher-order modes are lower than that of the plane wave in the clay medium. At high frequencies, the attenuation factors (Figure 2b) asymptotically approach and are always greater than the attenuation factor for the plane wave in the sand medium. At low frequencies, the attenuation factors for the higher-order modes become larger than that for the plane wave in the clay medium; in contrast, the attenuation factor for mode 0 decreases while always remaining larger than that of the plane wave in the sand medium. At high frequencies, the

phase velocities (Figure 2c) asymptotically approach and are always greater than the phase velocity of the plane wave in the sand medium. At low frequencies, the phase velocities for the higher-order modes become very large but remain finite; in contrast, the phase velocity for mode 0 decreases to less than that of the plane wave in the sand medium. The residues for E_z (Figure 2d) were calculated for the transmitting and the receiving antennas in the exact middle of the sand layer and separated by 10 m. For this geometry, only the even-number modes are excited; the reason will be given when the mode shapes are discussed. To prevent the product $I(\omega)\, ds$, which is needed to calculate the electric dipole moment and hence the residue, from complicating the interpretation of the residue, the product was set to 1 A-m for all frequencies. The significant contributions to E_z come from only mode 0 at low frequencies but from modes 0, 2, and 4 at high frequencies.

Only when the residue is large — for this example, large could be defined as any value greater than, say, 10^{-2} V/m — the energy velocity of the mode is just slightly less than the energy velocity of the plane wave in the sand medium, the attenuation factor is somewhat greater than the attenuation factor of the plane wave in the sand medium, and the phase velocity is practically constant. Since a guided wave is a weighted sum of modes, the guided wave will have the same behavior. Furthermore, because of the constancy of the phase velocity, the guided wave after transformation to the time domain will have little dispersion.

To show the shape of the modes, the real part of E_z was chosen because E_z is detected by the receiving antenna. The shapes for the even-numbered modes are symmetric about the middle of the sand layer (Figure 3); the shapes for the odd-numbered modes are anti-symmetric. The number of maxima and minima within the sand layer equals the mode number plus one; for example, mode 4 has 5 maxima and minima within the sand layer. With this simple formula the approximate shapes of any higher-order modes can be readily sketched. Although E_z is discontinuous at the clay-sand interfaces, the boundary conditions related to the current density (Stratton, 1941, p. 483) are satisfied. The real part of E_z is always greatest in the sand layer and decays very rapidly in the clay layers. For all of the shapes examined in this investigation, the real parts of E_z at a distance of approximately four or five skin depths into the clay were negligibly small compared to their values at the interface. For mode 0, which usually makes the largest contribution to the guided wave, the polarity of E_z in the clays is opposite that in the sand; this change will be evident in calculated radar scans if their amplitudes are normalized. The mode shapes change somewhat with frequency; but their symmetry and other properties do not.

The contribution that a mode mades to the guided wave depends, in part, upon the positions of the transmitting and the receiving antennas. If the transmitting antenna is placed where the magnitude of the field associated with a mode is zero, then that mode cannot be excited. Similarly, if the receiving antenna is placed there, the mode cannot be detected. For this reason, the anti-symmetric modes had zero residues when the transmitting and the receiving antennas were in the exact middle of the sand layer. On the other hand, if the transmitting antenna is placed where the magnitude of the field associated with a mode is non-zero, then that mode will be excited. Similarly, if the

receiving antenna is placed there, the mode (if present) will be detected. Because all antennas, in practice, have finite length, many modes will be excited, and those that are not attenuated too much will be detected.

3.2 Effects of the Sand Layer upon the Modes

In geologic and hydrologic investigations, at least three properties of the sand layer could be important: (1) the presence of an electrically conductive fluid or of significant amounts of clay particles, (2) the layer thickness, and (3) the presence of a fluid having a dielectric permittivity signficantly different from that of water (like a surfactant or a non-aqueous phase liquid) or a change in the water saturation. In terms of the model used here, these three properties affect (1) the electrical conductivity, (2) the thickness, h, and (3) the dielectric permittivity, respectively, of the sand layer. The effects of these three model parameters will be analyzed in this section. The analysis will not involve every mode and every mode property: Only modes 0 and 1 will be examined because the generalizations developed for these two will also apply to all of the higher-order modes; only the energy velocity and the attenuation factor will be examined because these two determine the most important properties of the guided wave: its travel time and, in part, its amplitude.

To determine the effects of the conductivity, the mode properties were calculated and analyzed for many different values of conductivity that were small enough to cause only insignificant velocity dispersion. The most important effect was found to be upon the attenuation factors of the modes at high frequencies (where the residue is large): The attenuation factors increase as the electrical conductivity increases (Figure 4); the increase for the attenuation factors is readily predictable because the asymptote, which is the attenuation factor for a plane wave in an infinite, homogeneous sand medium, also increases. Changes in the conductivity had no significant effect on the energy velocities.

To determine the effects of the dielectric permittivity, mode properties were calculated for several different values of it. Shown in Figure 5 are the mode properties for a model with a high permittivity and for another model with a low permittivity. At high frequencies, the energy velocities increase as the dielectric permittivity decreases; the increase is readily predictable because the asymptote, which is the energy velocity for a plane wave in an infinite, homogeneous sand medium, also increases. For both the energy velocity and the attenuation factor, the frequencies at which particular features occur — for instance, the frequencies of the maximum attenuation factors for mode 0 — shifts to higher frequencies as the permittivity decreases. (Also note that the attenuation factors for the plane wave in the sand medium increase as the permittivity decreases; this behavior is expected because the attenuation factor for a plane wave is inversely proportional to the square root of the dielectric permittivity (Stratton, 1941, p. 277). This phenomenom is related to the slight increase in the attenuation factors for the modes at high frequencies.)

To predict quantitatively and quickly the effects of the dielectric permittivity as well as the layer thickness, normalized variables may be used. These normalizations were found to work well:

$$f_n = \frac{fh}{v_p}, \tag{11}$$

$$v_{en} = \frac{v_e}{v_p}, \text{ and} \tag{12}$$

$$\alpha_n = \alpha h. \tag{13}$$

The frequency is f; the phase velocity of the plane wave in the infinite, homogeneous sand medium is v_p; and the attenuation factor is α. These normalization were applied to the mode properties for which the permittivity was changed (Figure 5) and mode properties for which the thickness was changed. The normalized mode properties (Figure 6) are similar, indicating that the normalizations account for the most important effects upon the modes.

To predict the effects of the dielectric permittivity on the modes, this parameter must be related to the normalized variables. The relation will be made with the phase velocity of the plane wave in an infinite, homogeneous sand medium:

$$v_p \cong \frac{c}{\sqrt{\varepsilon_{r2}}} \tag{14}$$

(Stratton, 1941, p. 274-277) where c is the speed of light in free space. (This equation is appropriate when the electrical conductivity of the sand is small.) For the effects of the permittivity upon the energy velocity, substitute equation 14 into equation 12:

$$v_{en} \cong \frac{v_e\sqrt{\varepsilon_{r2}}}{c}. \tag{15}$$

To predict, for example, an asymptotic velocity, note that the normalized value is 1 (Figure 6). When ε_{r2} is 20, the asymptotic velocity is calculated with equation 15 to be 0.67×10^8 m/s (see Figure 5). (The effects of the permittivity upon the phase velocities of the modes may be predicted in a similar manner.) For the effects of the permittivity upon the frequencies, substitute equation 14 into equation 11:

$$f_n \cong \frac{f h\sqrt{\varepsilon_{r2}}}{c}. \tag{16}$$

To predict, for example, the frequency at which the energy velocity of mode 0 is very close its asymptotic value, note that the normalized frequency at which this occurs is approximately 2 (Figure 6). When ε_{r2} is 10 and h is 1 m, the frequency of interest is calculated with equation 15 to be 190 MHz (see Figure 5).

The effects of the thickness of the sand layer can also be determined and predicted with the normalized variables. First, equation 13 shows that, for a given normalized attenuation factor, as the thickness decreases the attenuation factor increases. To predict, for example, the maximum attenuation factor for mode 0, note that its normalized value is approximately 0.5 (Figure 6). When the thickness is 0.5 m, the attenuation factor is calculated with equation 13 to be 1 Np/m. Second, equation 11 shows that, for a given normalized frequency, as the thickness decreases the frequency increases. In other words, the frequencies at which particular mode properties occur shift in a manner analogous to that caused by changes in the permittivity. Equation 11 can be used to predict those frequencies as was done for the permittivities.

3.3 Radar Scans

In this subsection radar scans for several different configurations of the transmitting and the receiving antennas, configurations that could be used in the field, are presented and analysed. The effects of the antenna configuration and the geology upon the radar waves is the focus of the analysis. For the guided wave this analysis will involve the properties of the modes, which were presented in the last two subsections.

The scans were calculated for a model representing saturated sediments (Table 1), the same model used to calculate the properties of the modes. The electrical current $I(t)$, which drives the transmitting antenna, was chosen to be a Ricker wavelet:

$$I(t) = \frac{1}{4\sqrt{\pi}}\left[1 - \frac{1}{2}(2\pi f_o)^2 (t - t_o)^2\right] e^{-\frac{1}{4}(2\pi f_o)^2 (t - t_o)^2} \text{ A}, \tag{17}$$

where f_o, the center frequency, was chosen to be 100 MHz, and t_o, the time shift, was chosen to be 12.33 ns. Because of the time shift, which is needed to make the simulation causal, the wavelet is practically zero for approximately 3 ns (Figure 7a). In the frequency domain (Figure 7b), the amplitudes are significant between approximately 10 and 250 MHz, which is typical of some existing radar systems.

The first set of calculated scans (Figure 8) show how increasing the distance between antennas, which would occur if the distance between wells increased, affects the radar waves. The transmitting and the receiving antennas were located in the exact middle of the sand layer and were separated by 5, 10, and 15 m. The contributions from the direct and the guided waves were computed and displayed separately to make comparsions easy. For the direct wave, the amplitude decreases as the distance increases primarily because of geometric spreading; no dispersion is evident. For the guided wave, the amplitude also decreases as the distance increases primarily because of geometric spreading and attenuation caused by the electrical conductivity of the clay layers. The dispersion is minor but obvious; such a small amount was expected because the phase velocities of the modes are practically constant when their residues are large (Figure 2c). At each receiving antenna, the direct wave arrives just before the guided wave because the energy velocity

of the direct wave, which depends upon the properties of the sand, is just slightly greater than the energy velocity of the modes when their residuals are large (Figure 2a). The difference in time is small compared to the duration of both waves, and consequently the waves will overlap each other when they are summed. Because the shape of the direct wave, after changing its polarity, is almost identical to that of the first part of the guided wave, they will cancel somewhat when they are summed, making the maximum amplitude of the complete wave smaller; this point is illustrated in the next example.

For the remaining sets of scans, the complete wave — the sum of the direct and the guided waves — is displayed, as only it is detected by the receiving antenna. The second set of scans (Figure 9) show how the radar waves are affected by the strata when the antennas move simultaneously up the wells, a configuration often used in the field. The scans were computed with the antennas separated by 10 m and at equal heights of -0.6 m, -0.4 m, -0.2 m, etc. (The scan at a height of 0.0 m is the sum of the scans for the direct and the guided waves at 10 m in Figure 8.) The amplitude of the radar wave is greatest when the antennas are in the middle of the sand layer, and the amplitude decreases as the antennas approach either the top or the bottom of the sand layer. The decrease is not caused by the direct wave — it remains the same at all heights. Rather, it is caused by the guided wave: as the heights of the transmitting and the receiving antennas change, the residues for the modes change because the extents to which the modes are excited and are detected change. In the sand layer, the travel time of the wave is constant, 152 ns. When the antennas are in either clay layer, the amplitude of the radar waves are very small because the electrical conductivity greatly attenuates the direct wave, and the transmitting and the receiving antennas poorly excite and poorly detect, respectively, the modes.

The third and last set of scans (Figure 10) show how the radar waves are affected by the strata when one antenna is fixed and the other moves up the well, a configuration often used for tomography. The scans were computed with the antennas separated by 10 m, with the transmitting antenna fixed at a height of 0.0 m, and with the receiving antenna at heights of -0.6 m, -0.4 m, -0.2 m, etc. (The scan for the receiving antenna at a height of 0.0 m is the same as the scan at the height of 0.0 m in Figure 9.) The amplitude of the radar wave is greatest when the receiving antenna is in the middle of the sand layer, the amplitude decreases as the antenna approaches either the top or the bottom of the sand layer. This decrease is not caused by the direct wave because it practically does not change. Rather, it is caused by the guided wave: as the height of the receiving antenna changes, the residues of the modes change because extents to which the modes are detected change. When the receiving antenna is in either clay layer, the amplitude of the radar wave is very small.

The significant differences between the radar scans displayed in Figures 9 and 10 are their amplitudes (except for the scan at a height of 0.0 m). This differences are caused by the transmitting antenna: for the scans in Figure 9, it moved, changing the excitation of the modes; whereas for the scans in Figure 10, it was fixed keeping the excitation of the modes constant.

4. DISCUSSION

Frequency dependence in the constitutive parameters was omitted because it would complicate the intepretation of the results. Nonetheless, such dependence could be easily incorporated into the solutions because they are formulated in the frequency domain — the only changes are replacing (pure real) ε_r with (complex) $\varepsilon_r(\omega)$ and (pure real) μ_r with (complex) $\mu_r(\omega)$. (The effects of frequency on the conductivity are accounted for by the imaginary part of $\varepsilon_r(\omega)$ (Balanis, 1989, p. 77).) Although the effects of frequency dependence have not been formally computed yet, they may be readily predicted: Because the real part of the permittivity generally tends to decrease as the frequency increases (see, for example, Hoekstra and Delaney, 1974), the energy and the phase velocities of the guided and the direct waves will probably increase. From an asymptotic analysis of the wave number for a plane wave — an analysis similar to that given by Stratton (1941, p. 276-277) — the real part of the wave number is found to be affected more by the real part of the permeability than by the imaginary part. Because the real part of the permeability tends to decrease as the frequency increases (see, for example, Olhoeft and Capron, 1993), the wave number will decrease, but the energy and the phase velocities of the plane wave will increase. Consequently, the energy and the phase velocities of the guided and the direct waves will probably increase. From a similar asymptotic analysis, the imaginary part of the wave number for a plane wave is found to be affected more by the imaginary parts of the permittivity and permeability than by the real parts. Because the imaginary part of the wave number determines the attenuation of the plane wave, non-zero imaginary parts of the permittivity and permeability will probably increase the attenuation of the guided and the direct waves beyond that caused by the conductivity.

Of the existing methods to process cross-well radar data (as well as cross-well seismic data), travel-time tomography and attenuation tomography are the most common. For good spatial resolution of the tomography results, the rays representing the waves must crisscross each other at many different angles in the region between the wells (Bregman and others, 1989). To have such ray coverage, radar waves must be detected for many, many different locations of the transmitting and the receiving antennas. A problem occurs when both antennas are within the same, continuous clay layer (see, for example, Figure 9); the attenuation may be so great that the radar wave would be undetectable. A similar problem occurs when either one antenna is within a clay layer (see, for example, Figure 10) or when a clay layer separates the antennas. Again the radar wave would be undetectable. In either case, the consequence for tomography is that, because a significant portion of the rays would be missing, the tomography results would have poor spatial resolution.

An alternative to tomography is simply displaying the radar scans. For example, the scans can be plotted between the wells — the start of the scan is at the height of the transmitting antenna and the end of the scan at the height of the receiving antenna. With this display, the character of the scans in conjunction with other geologic and geophysical information, can be readily analyzed to make a qualitative interpretation. With such an analysis, the continuity of a sand or a gravel layer between wells should be apparent; this approach is

akin to cross-well continuity logging, which is being used in the oil industry (see, for example, Lines and others, 1992; Krohn, 1992). Another alternative to tomography is picking the travel times. When the antennas are at the same height, the picks can be used to estimate an bulk, relative dielectic permittivity for the sediments at that height. To demonstrate this estimation, it was applied to the scans in Figure 9: Using 152 ± 1 ns as the travel time and its approximate error and using 3 ns as the approximate delay of the transmitting antenna (Figure 7a), the relative permittivity was calculated to be 20.0 ± 0.3, which equals, within the margin of error, the exact value for the sand layer (Table 1).

Although the amplitudes obviously contain information about the layers (Figures 9 and 10), extracting that information is not straightforward: the amplitudes are affected by the layer in which the antennas are located as well as by the other, nearby layers. For instance, in Figure 9, the amplitudes of the scans from the top or the bottom of the sand layer are much lower than the amplitudes of the scans from the middle. This difficulty could be overcome using full-waveform inversion, which would account for the effects of nearby layers, but before such a sophisticated method is tried the simplier methods should be perfected.

5. CONCLUSIONS

Radar wave propagation in layered sediments was simulated with a model having three layers: clay, sand, and clay. In the layer containing the transmitting antenna, part of the field is a wave radiated from that antenna. The other part, which exists in the other layers too, is a wave related to the interaction of the field with the three layers; for the model used here this field propagates as if it were guided by the sand layer. In the frequency domain, this guided wave may be represented as a weighted sum of modes.

The properties of the modes were calculated for a model representing saturated sediments. At high frequencies, the energy velocity and the attenuation factor of a mode asymptotically approach the energy velocity and the attenuation factor, respectively, of a plane wave in an infinite, homogeneous medium having the constitutive parameters of the sand layer. Furthermore, at high frequencies, the phase velocity is practically constant. The residues were only examined for the antennas are in the middle of the sand layer; for this configuration the residue for mode 0 at high frequencies is the largest; for mode 2 the next largest; etc., and the residues for the odd-numbered modes are all zero. For each mode the electromagnetic fields have a characteristic spatial pattern or shape; this shape determines the extent to which the mode may be excited by the transmitting antenna or detected by the receiving antenna. The shapes of the modes show that the fields are always largest in the sand layer and decay very rapidly in the clay layers.

The properties of the sand layer are strongly affect the mode properties: As its electrical conductivity increases, the attenuation factors at high frequencies (where the residues are large) increase. As its dielectric permitivity decreases, the frequency range for a mode shifts to higher frequencies, and the energy velocities at high frequencies (where the residues are large) increase. As its thickness decreases, the frequency range for a mode

shifts to higher frequencies, and the attenuation factor increases. The effects related to changes in dielectric permittivity and thickness can be quickly predicted using normalized variables.

For the model representing saturated sediments, radar scans were calculated for different configurations of antennas that are commonly used to aquire data. When both antennas were both in the middle of the sand layer and the distance between them increased, the character of the guided wave changed only slightly because its dispersion was small. At all offsets, the travel time of the guided wave was just slightly greater than that of the direct wave, within the accuracy of the travel time picks. When the heights of the antennas changed simultaneously the radar wave was strongly affected by the layers: When the antennas were both in a clay layer, the amplitude of the wave was very small. However, as the antennas moved through the sand, the amplitude increased from a minimum near the sand-clay interface to a maximum in the middle. The travel time of the wave was constant. When the transmitting antenna was fixed in the sand layer and the receiving antennas was moved, the results related to the amplitudes were generally similar to those obtained when the heights of both antennas changed simultaneously.

The results indicate that cross-well radar data collected in layered sands and clays probably cannot be processed with tomographic methods because the clays will significantly attenuate the waves propagating across the layers, making the resolution of the tomogram poor. The data probably can be processed with a modification of cross-well continuity logging, which was developed for cross-well seismic data. When a radar wave is detectable, its travel time can be directly related to the bulk dielectric permittivity of the layer in which the antennas are located. Using the amplitude of the wave to estimate sediment properties will require some sophisticated processing as the amplitude is affected by the other, nearby layers.

6. ACKNOWLEDGEMENTS

D. V. Fitterman made many suggestions that improved this manuscript. This work was sponsored by the Department of Energy under Interagency Agreement DE-AI09-91SR18222.

7. REFERENCES

Balanis, C. A., 1989, Advanced engineering electromagnetics: New York, John Wiley & Sons, Inc., 981 p.

Bregman, N. D., Bailey, R. C., and Chapman, C. H., 1989, Ghosts in tomography: The effects of poor angular coverage in 2-D seismic traveltime inversion: Canadian Journal of Exploration Geophysics, vol. 25, p. 7-27.

Bouchon, M., 1981, A simple method to calculate Green's functions for elastic layered media: Bulletin of the Seismological Society of America, v. 71, no. 4. p. 959-971.

Churchill, R., V., Brown, J. W., and Verhey, R. F., 1960, Complex variables and applications: New York, McGraw-Hill, Inc., 332 p.

Collin, R. E., 1991, Field theory of guided waves: New York, IEEE Press, 852 p.

Ellefsen, K. J., 1996a, Cross-well radar: A feasibility test at the M-Area basin, Savannah River Site, South Carolina: U. S. Geological Survey Open File Report, *in preparation.*

Ellefsen, K. J., 1996b, Summary of geophysical investigations in support of DNAPL remediation at Savannah River Site, South Carolina: U. S. Geological Survey Administrative Report, *in preparation.*

Fuller, J. A., and Wait, J. R., 1976, A pulsed dipole in the Earth, *in* Felsen, L. B., ed., Transient electromagnetic fields: Topics in Applied Physics, v. 10, p. 237-269.

Greenhouse, J., Brewster, M., Schneider, G., Redman, D., Annan, P., Olhoeft, G., Lucius, J., Sander, K., and Mazzella, A., 1993, Geophysics and solvents: The Borden experiment: The Leading Edge, vol. 12, no. 4, p. 261-267.

Hoekstra, P., and Delaney, A., 1974, Dielectric properties of soils at UHF and microwave frequenecies: Journal of Geophysical Research, v. 79, no. 11, p. 1699-1708.

Jordan, J. E., Looney, B. B., Rossabi, J., Bergren, C. L., 1993, Savannah River Site DNAPL Technical Program Plan, Report No. WSRC-TR-93-606, Westinghouse Savannah River Company, Aiken, SC 29808.

Lines, L. R., Kelly, K. R., Queen, J., 1992, Channel waves in cross-borehole data: Geophysics, v. 57, no. 2, p. 334-342.

Krohn, C., 1992, Cross-well continuity logging using guided seismic waves: The Leading Edge, vol. 11, no. 7, p. 39-45.

Olhoeft, G. R., Capron, D. E., 1993, Laboratory measurements of the radiofrequency electrical and magnetic properties of soils from near Yuma, Arizona: U. S. Geological Survey Open File Report 93-701, 214 p.

Stratton, J. A., 1941, Electromagnetic theory: New York, McGraw-Hill, Inc., 615 p.

Tyras, G., 1969, Radiation and propagation of electromagnetic waves: New York, Academic Press, 368 p.

Wait, J. R., 1962, Electromagnetic waves in stratified media: New York: MacMillian Co., 372 p.

Westinghouse Savannah River Company, 1992, Assessing DNAPL contamination, A/M-area, Savannah River Site: Phase I results, Report No. WSRC-RP-92-1302, available from Environmental Sciences Section, Westinghouse Savannah River Company, Aiken, SC 29808.

Wright, D. L., Grover, T. P., Ellefsen, K. J., Lane, J. W., Jr., Kase, P. G., 1996, Radar tomograms at Mirror Lake, New Hampshire: 3-D visualization and a brine tracer experiment: Proceedings of the Symposium on the Application of Geophysics to Engineering and Environmental Problems, Keystone, Colorado, Environmental and Enginering Geophysical Society, p. 565-575.

Table 1. Values used for the model representing saturated sediments.

Model Parameter	Layer 1 (Lower Clay Layer)	Layer 2 (Sand Layer)	Layer 3 (Upper Clay Layer)
Relative Dielectric Permittivity	40	20	40
Relative Magnetic Permeability	1	1	1
Conductivity	0.5 S/m	0.0001 S/m	0.5 S/m
Thickness	-	1 m	-

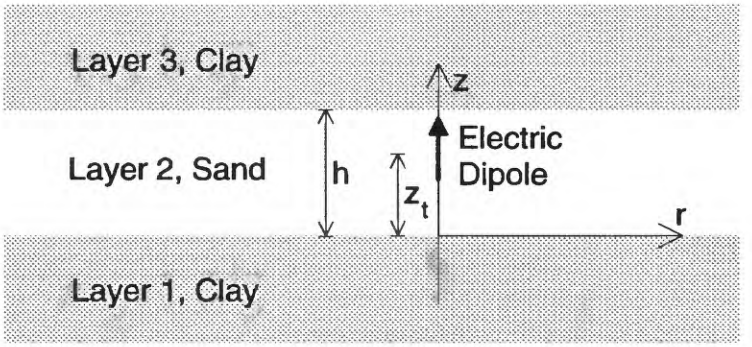

Figure 1. Model used to simulate radar wave propagation in layered sediments. Layers 1 and 3 are half-spaces. The symbols are explained in the text.

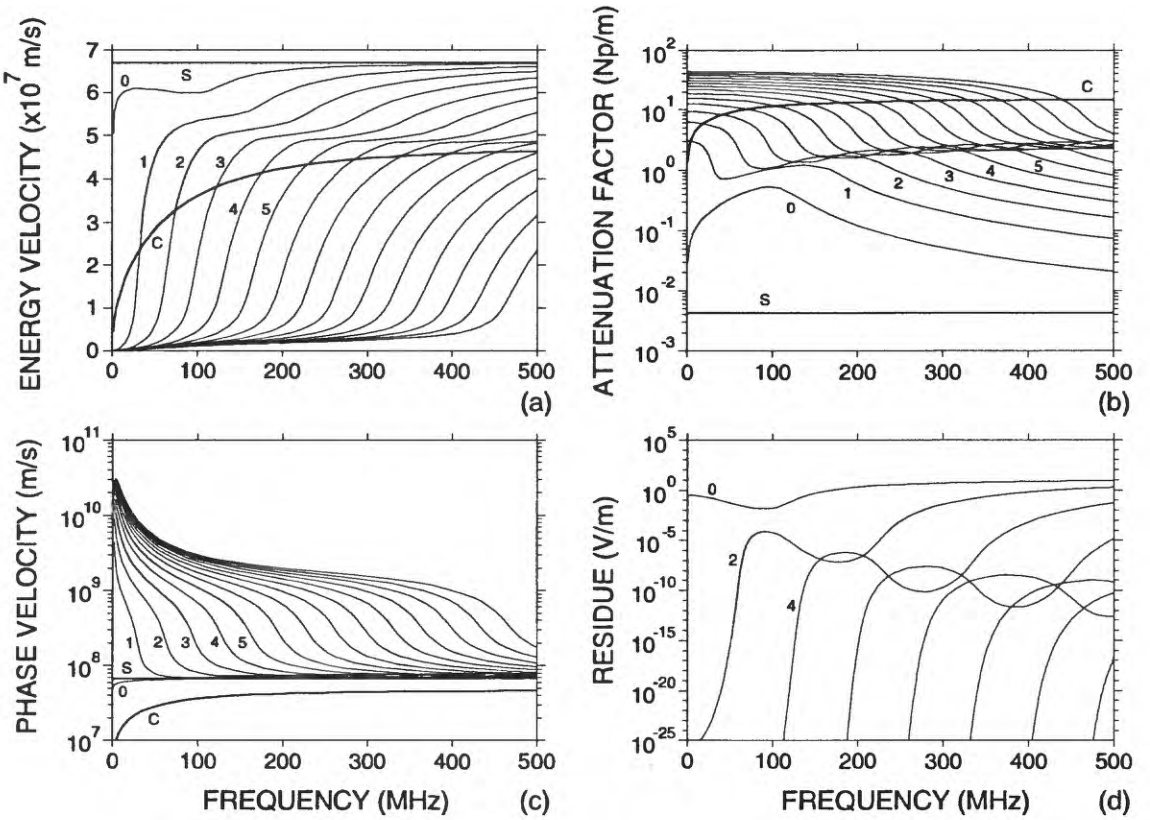

Figure 2. Properties of the modes. (a) Energy velocities. (b) Attenuation factors. (c) Phase velocities. (d) Residues. These properties were calculated for layered, saturated sediments represented by the model shown in Figure 1. Only the lowest-order modes are labeled. In (a), (b), and (c) each thick line represents the equivalent property of a plane wave propagating in an infinite, homogeneous medium. For the thick line labeled "S," the medium is sand; for the thick line labeled "C," clay. The properties of the sand and clay are given in Table 1.

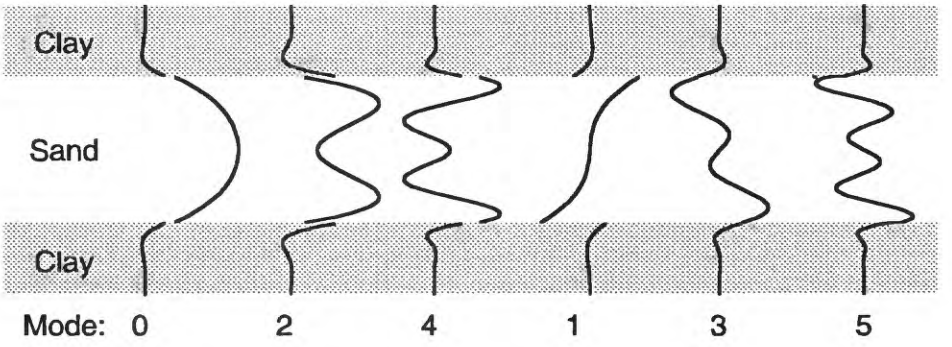

Figure 3. Mode shapes showing the vertical component of the electric field.

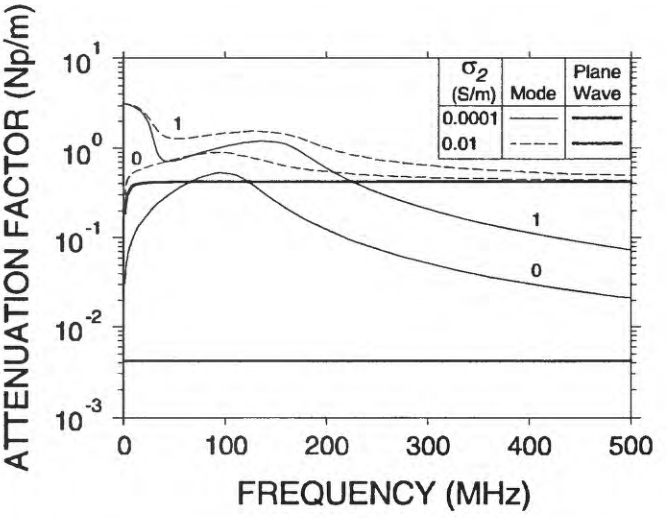

Figure 4. Effects of changes in the electrical conductivity of the sand layer upon the attenuation factors of modes 0 and 1. The thin lines pertain to the modes; the thick lines to plane waves propagating in infinite, homogeneous sand media. The electrical conductivies for the sands are given in the legend; all other properties are given in Table 1.

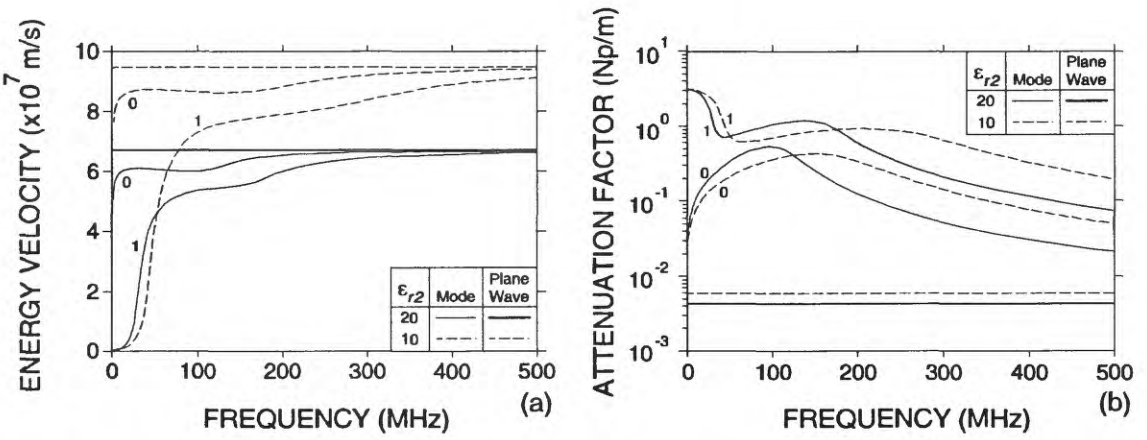

Figure 5. Effects of changes in the dielectric permittivity of the sand layer upon (a) the energy velocities and (b) the attenuation factors of modes 0 and 1. The thin lines pertain to the modes; the thick lines to plane waves propagating in infinite, homogeneous sand media. The relative dielectric permittivities for the sands are given in the legend; all other properties are given in Table 1.

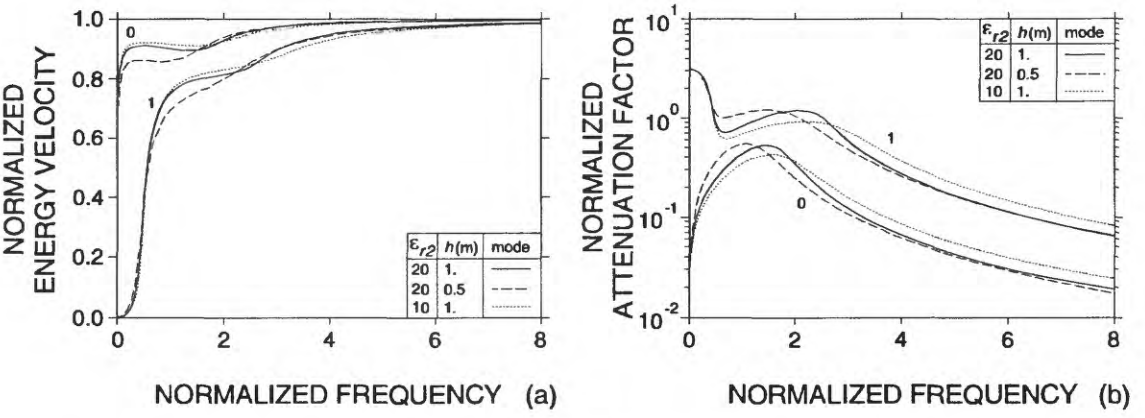

Figure 6. (a) Normalized energy velocities and (b) normalized attenuation factors for models in which the dielectric permitivitty and the thickness of the sand layer were changed. The values used for these two parameters are given in the legend; all other properties are given in Table 1. The normalization is explained in the text.

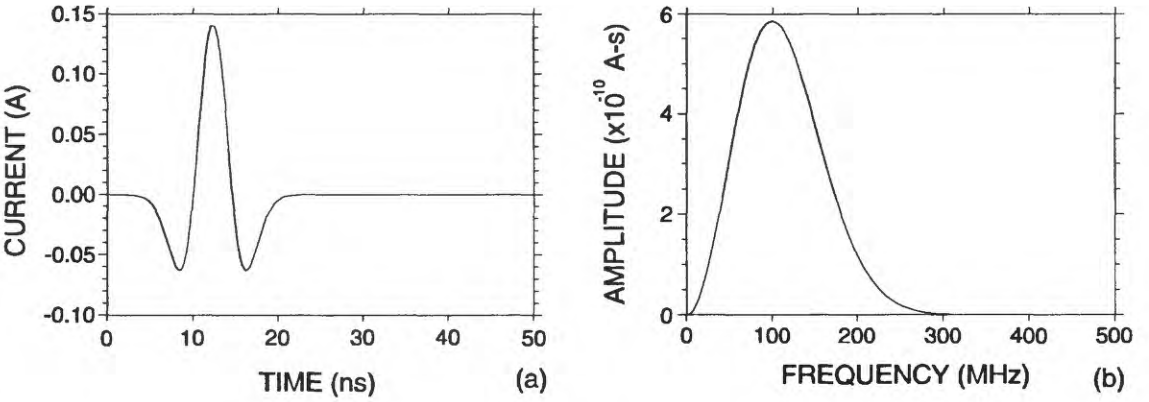

Figure 7. (a) Electrical current used to drive the transmitting antenna. (b) Amplitude of the current in the frequency domain.

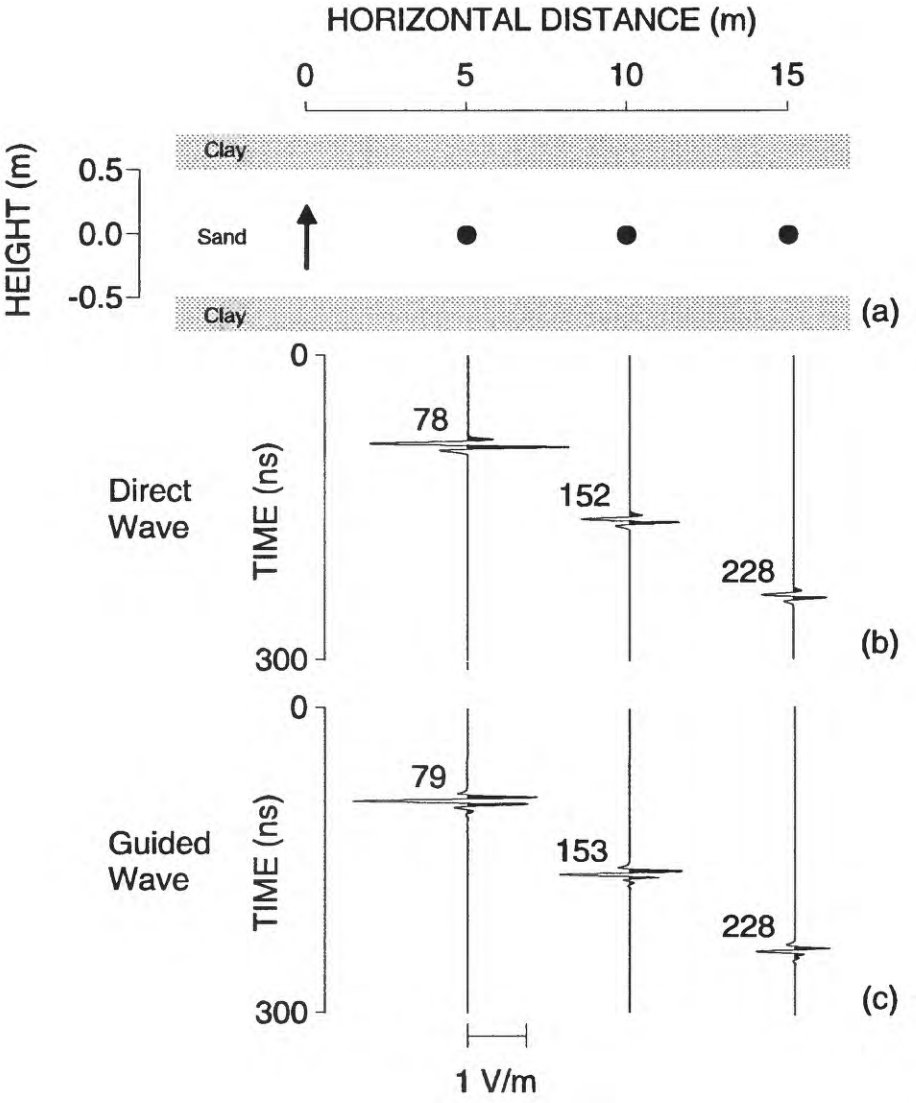

Figure 8. Effects of increasing the distance between the antennas upon the direct and the guided waves. (a) The model, for which the vertical exaggeration is 4, and the locations of the antennas. The clay layers are half-spaces. The arrow represents the transmitting antenna; the circles represent the different locations of the receiving antenna. (b) Direct waves. (c) Guided waves. Next to each wave is its travel time (in ns), for which the accuracy of the pick is approximately 1 ns. The amplitudes are proportional to the scale at the bottom.

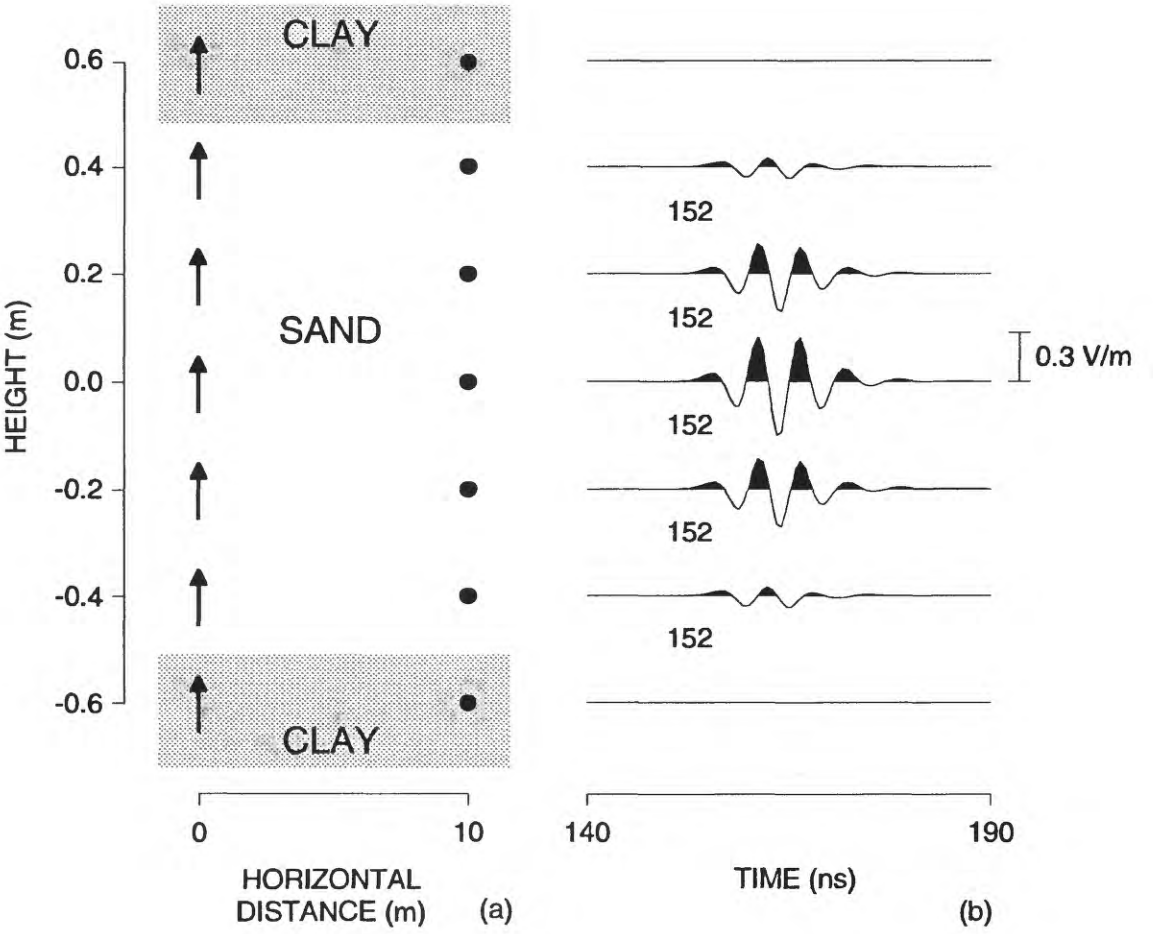

Figure 9. Effects of the layered sediments on the radar waves as both antennas move. (a) The model, for which the vertical exaggeration is 20, and the locations of the antennas. The clay layers are half-spaces. The arrows represent the successive locations of the transmitting antenna; the circles represent the successive locations of the receiving antenna. (b) Radar scans, for which the amplitudes are relative to the scale at the right. Next to each wave is its travel time (in ns), for which the accuracy of the pick is approximately 1 ns.

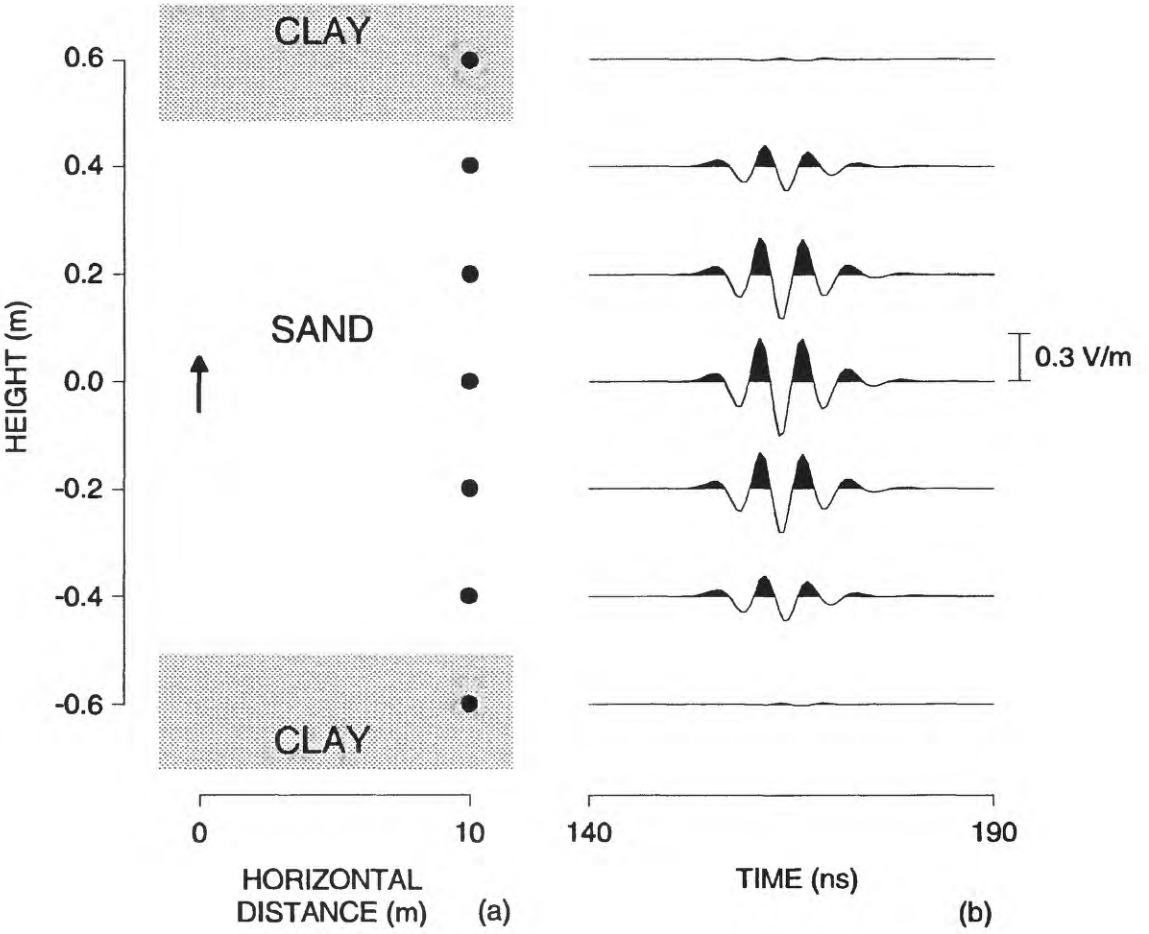

Figure 10. Effects of the layered sediments on the radar waves as only the receiving antenna moves. (a) The model, for which the vertical exaggeration is 20, and locations of the antennas. The clay layers are half-spaces. The arrow represents the transmitting antenna; the circles represent the successive locations of the receiving antennas. (b) Radar scans, for which the amplitudes are relative to the scale at the right.